Taylor dispersion of inorganic nanoparticles and comparison to dynamic light scattering and transmission electron microscopy

Author list

Dominic A. Urban†, Ana M. Milosevic†, David Bossert†, Federica Crippa†, Thomas L. Moore†, Christoph Geers†, Sandor Balog†, Barbara Rothen-Rutishauser, Alke Petri-Fink*†#

†AdolpheMerkle Institute, University of Fribourg, Chemin des Verdiers 4, 1700 Fribourg, Switzerland

#Chemistry Department, University of Fribourg, Chemin du Musée 9, 1700 Fribourg, Switzerland

*Corresponding Author : Adolphe Merkle Institute, University of Fribourg, Chemin des Verdiers 4, 1700 Fribourg,Switzerland.

email: alke.fink@unifr.ch

Supplementary data

Table of content:

EXPERIMENTAL SECTION

S1 Gold nanoparticle synthesis.

Citrate stabilized gold (Au) NPs were synthesized following well-documented synthesis methods. The small, approximately 15nm Au NPs (Au-M) were synthesized based on the method described by Turkevich et al.[1] Briefly, 500mL (0.5 mmol/L) chloroauric acid(HAuCl4)(Sigma Aldrich, St. Louis, USA) solution was brought to boil for approximately 10 min, prior to the addition of 25 mL (34 mmol/L) of a sodium citrate (Sigma Aldrich, St. Louis, USA) solution. The mixture was kept at boiling temperature for additional 20 min, before the mixture was removed from heat and left to cool to room temperature. The final NP suspension was stored in the dark at a temperature of 5°C.

The larger, approximately 47nm sized particles (Au-L), were synthesized following the work of Brown et al.[2]. A 600mL aqueous solution of $HAuCL_4$ (0.25mM), and hydroxylamine hydrochloride (SigmaAldrich, St. Louis, USA) (1.96 mM) was prepared in a glass bottle and homogenized with a magnetic stirrer. The previously described Au-NPs were used as Au seed suspension (1.2 mL) and added to the mixture. The mixture was stirred constantly for approximately 20 min, during which time a color shift could be observed. The resulting NPs were stabilized by the addition of 7.14 mg of sodium citrate. NPs were purified by centrifugation (4000 rpm for 15 min) and re-dispersed in MilliQ water (Millipore purification system, Bedford, MA, USA).

The smallest Au NPs (Au-S) were synthesized via a method described by Yong et al.[3] For the synthesis, 46 mL of MilliQ water, 0.5 mL of 1 mol/L sodium hydroxide solution, and 1 mL of a Tetrakis(hydroxymethyl) phosphonium chloride (THPC) solution (12 µL of 80% THPC in 1 mL of MilliQ water) were homogenized. Consequently 10 mL of a 5 mmol/L $HAuCl_4$ was added under stirring, and the solution was left to react for several minutes, resulting in ultrasmall Au NPs. The synthesized particles were characterized immediately after synthesis.

S2 Superparamagnetic iron oxide NP (SPION) synthesis.

The iron oxide NPs with approximate diameters of 13 (SPIONs-S) and 24 nm (SPIONs-L) were synthetized by thermal decomposition, based on the method described by Park et al. [4] An iron oleate, obtained by reacting iron-III-chloride (FeCl3·6H2O) (Sigma Aldrich, St. Louis, USA) and sodium oleate (Sigma Aldrich, Sl. Louis, USA) was heated to 320 °C, in the presence of oleic acid (Sigma Aldrich, Sl. Louis, USA). A well-defined temperature ramp was applied to keep the mixture boiling for a defined time period depending on the desired NP size (30min for the 13 nm particles and 1h for the 24 nm particles). After particle formation the solution was quickly cooled to room temperature and purified via centrifugation. The oleic acid stabilized NPs were transferred to different solvents (hexane, chloroform, and toluene) and stored at 4°C, prior to further functionalization. In order to transfer the NPs to water, the surface grafted oleate was exchanged by citric acid (Sigma Aldrich, St. Louis, USA), as previously described [5].

S3 Silica NP synthesis.

The silica (SiO_2) NPs were synthesized using two different methods described in the literature. The smaller NPs, approximately 20 nm (SiO_2-S), were synthesized using the biphasic synthesis described by Hartlen et al [6]. The synthesis was performed in a 20 mL vial. 14.7 mg of arginine (Sigma Aldrich, St. Louis, USA) was weighed and dissolved in 6.9 mL of MilliQ water. The solution was transferred to a vial and 0.45 mL cyclohexane (Acros Organics New Jersey, USA) was added. The reaction was heated to 60 °C in an oil bath under magnetic stirring. The mixing was adjusted to make sure that the top layer of cyclohexane remained relatively undisturbed. Once the solution had reached 60 °C, 0.55 mL of tetraethyl orthosilicate (TEOS) (Sigma Aldrich, St. Louis, USA) was slowly added to the vial so the TEOS was separated from the aqueous solution by the cyclohexane. The reaction was then kept at constant stirring and temperature for 24h.The cyclohexane was removed from the reaction mixture by gentle evaporation under reduced pressure. The remaining reaction mixture was transferred to a dialysis tube and submersed in a large beaker filled with MilliQ water. The water was continuously stirred and refreshed over the course of a few days.

The two larger particles were synthesized (SiO_2-M, SiO_2-L) following a modified procedure of the Stöber synthesis, described by Giesche et al.[7] A mixture of ethanol (208 mL for SiO_2-M, 161 mL for SiO_2-L), MilliQ water (13.5 mL for SiO_2-M, 58,5 mL for SiO_2-L), and ammonia (7.8 mL) (VWR, Dietikon, Switzerland) were transferred to a round bottom flask, in an oil bath, and stirred with a magnetic stirrer. TEOS (23 mL for SiO_2-M, 22.2 mL for SiO_2-L) was transferred rapidly to the round bottom flask and continuously stirred for approximately 4 hours. The middle sized SiO2 particles had additional dye molecules incorporated into the silica matrix, by adding (3-Aminopropyl)triethoxysilane 6 µL, modified with Atto647 fluorescent dye (300 µL) (ATTO-TEC GmbH, Siegen, Germany) into the synthesis mix. Next the ethanol was removed from the suspension by evaporation under reduced atmosphere. Following the removal of ethanol, the suspension was transferred to a dialysis tube and submersed in a large beaker filled with MilliQ water. The water was continuously stirred and refreshed over the course of 3 few days.

S4 Taylor Dispersion Analysis experimental setup.

Sizing experiments were performed using an ActiPix D100 UV-Vis area imaging detector (Paraytec,York, UK,20 Hz sample rate). The detector uses a sensor array, with 1280 columns by 1024 rows, giving a total of 1.3 mega pixels. Each pixel has a size of seven by seven micrometers, so a total of 49 μm^2 is imaged. The advantages of this area detector are the possibility to bin pixels, in case sample concentrations or detection limits are low. Additionally, the array detector enables the selective detection of only the center of the capillary, by comparing each pixel of the capillary area with reference pixels outside of the capillary. This prevents scattering and false signals to occur due to light scattering at the capillary walls. Depending on the analyte, either a 214 nm (± 10 nm) bandpass filter, a 280nm (± 10 nm) bandpass filter, a 400nm (± 10 nm) bandpass filter or a 520 nm (± 10 nm) bandpass filter (Edmund Optics, York, UK) coupled with a neutral density filter (10% transmission) (Edmund Optics, York, UK) were used. NPs suspensions were injected into a fused silica capillary (Polymicro Technologies, Phoenix, USA) under continuous flow conditions, using a capillary electrophoresis injection system (Prince 560 CE Autosampler, Prince Technologies B.V., Netherlands). The total capillary length (74.5 µm inner diameter) was 130 cm, with the length to the end of the first window being 45 cm and the length to the end of the second window being 85 cm, and a total window length of 1cm. The detector and capillary were placed inside of the injection system to allow for temperature regulation, which was kept constant at 25°C.

All samples were measured a minimum of three times under the same conditions. Depending on the measured signal intensity, varying injection volumes were used for the individual NPs or protein samples. After sample injection, a pressure of 70 mbar was applied to transport the NPs samples through the capillary, the injection volume was between 100-200 nL. For the silica NPs, BSA, the running buffer was MilliQ water. To prevent NP-capillary wall interactions a 0.001% (wt/V) TWEEN®20 (Sigma Aldrich, St. Louis, USA) solution was used as running buffer for the gold NPs and SPIONs. The data treatment was performed with an in house developed script for mathematica (Wolfram Research Inc.).

S5 Dynamic light scattering measurements.

All DLS measurements were performed on a commercial goniometer instrument (3D LS Spectrometer, LS Instruments AG, Switzerland). Samples were diluted in either water or a 0.001% (wt/V) TWEEN®20 solutions, depending on the running buffer used during TDA experiments, to insure that the samples were kept in the same matrix. Measurements were performed at multiple angles and repeated five times at each angle. The laser used was a Cobolt 05-01 diode pumped solid state laser (660 nm wavelength, max. power 500mW). The scattered light was collected and guided towards the detection system via single-mode optical fibers, equipped with integrated collimation optics. The signal light was coupled into two high-sensitivity APD detectors via laser-line filters (Perkin Elmer, Single Photon Counting Module), and a correlator (two-channel multiple-tau correlator) gathered the outputs and cross-correlated the two channels.

S6 Particle concentrations.

The particle concentrations used for the DLS and TDA analysis are the following: 2 g/L for the silica nanoparticles, 322 mg/L for the SPIONS-S, 366 mg/L for the SPIONS-L, 171 mg/L for the Au-S, 90 mg/L for the Au-M, 121 mg/L for the Au-L, and 5 g/L for the BSA system.

S7 TEM characterization.

Sample preparation for TEM analysis followed two different methodologies, depending on the analyzed sample. SiO_2 NPs and SPIONs were prepared by drop casting of a diluted particle suspension onto a TEM grid. The remaining NPs samples were prepared using a method described by Michen and Geers et al.[8] to prevent drying artefacts during the TEM sample preparation. In essence, NPs samples were dispersed in pre-sonicated BSA. As shown before, the BSA/NP ratio depends on NPs type, size and shape, and was calculated using an online calculator, provided at bsa.bionanomaterials.ch. After sample preparation, 5µL of the solution were deposited on a TEM grid and allowed to dry prior to TEM analysis. All images were acquired using an FEI Tecnai Spirit TEM with a Veleta2048 x 2048 wide angle CCD camera at 80 kV. The image analysis was performed using ImageJ as software.

S8 TDA analysis explained.

The Taylor Dispersion analysis performed in this project was performed as follows. After recording the TDA dispersion profiles at two detection windows along the capillary, a simple Gaussian fit, using least squares, is performed to gain the mean (t_1, t_2) and variance ($\sigma_1^{2\,s}$, σ_2^2) of the dispersion profiles. This is exemplary shown in the following two Taylorgrams, SI 2 and SI 3, where we analysed bovine serum albumin (BSA) and the gold particles, with an approximate TEM diameter of 15 nm. Following this, the mean and variance are used to solve the following two equations to obtain the diffusion coefficient and subsequently the hydrodynamic radius.

$$D = \frac{R_c^2(t_2 - t_1)}{24(\sigma_2^2 - \sigma_1^2)} \quad (1)$$

$$R_h = \frac{k_B T}{6\pi\eta D} \quad (2)$$

In the equations D is the diffusion coefficient, R_c the capillary radius, t_1 and t_2 are the average travel times of the dispersion profiles, and σ_1 and σ_2 are the standard deviations of the profiles at the first and second window respectively. k_B is the Boltzmann constant, T the temperature and η is the dynamic viscosity of the running buffer, and finally Rh stands for the hydrodynamic radius.

Since Taylor and Aris first described their theory, [9-11] more work has been done with respect to measurement boundary conditions, which must be met in order to perform TDA experiments. Alizadeh et al. for example described alternative conditions necessary to insure correct measurements,[12] in essence that Dt^2/R , where D is a particles diffusion coefficient, t the mean residence time, and R the inner radius of the capillary, be in some sense large. Bello et al and Belongia et al. stipulated that experimentally it is of greater importance for a

monodispersed spherical system to resemble a Gaussian function when passing the detection window to aptly estimate correct hydrodynamic sizes. [13, 14]

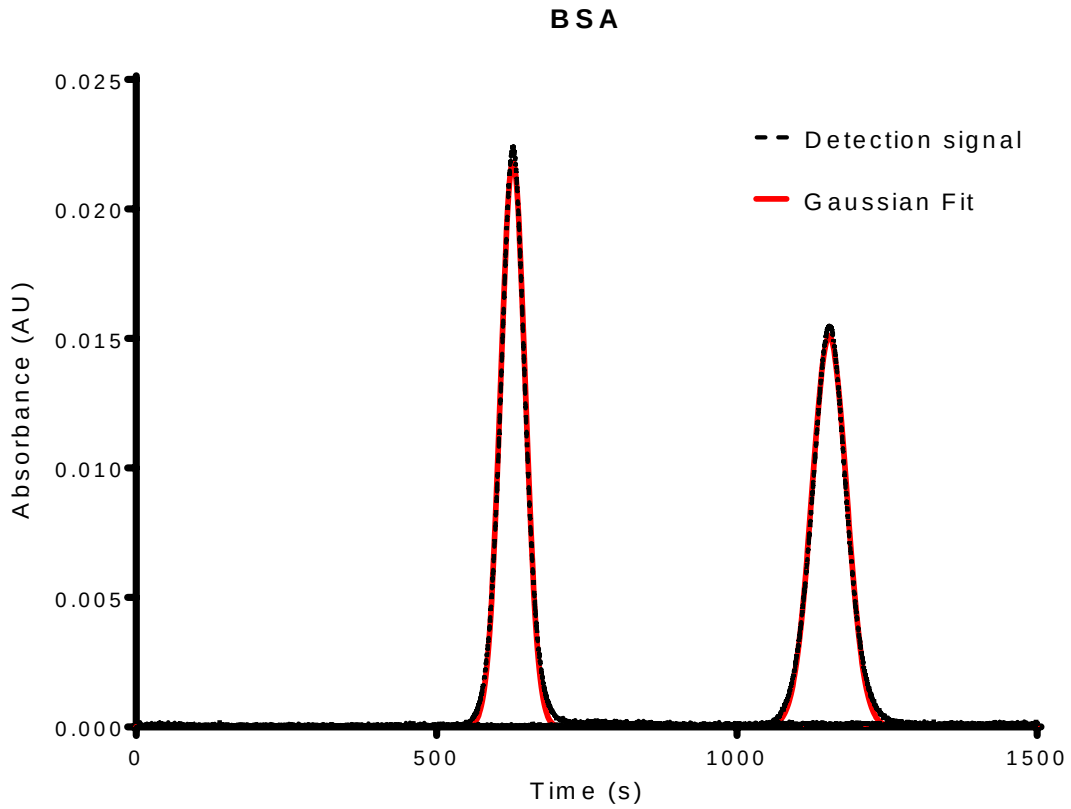

S9 Taylorgram and Gaussian fit of the bovine serum albumin sample, measured at 214 nm.

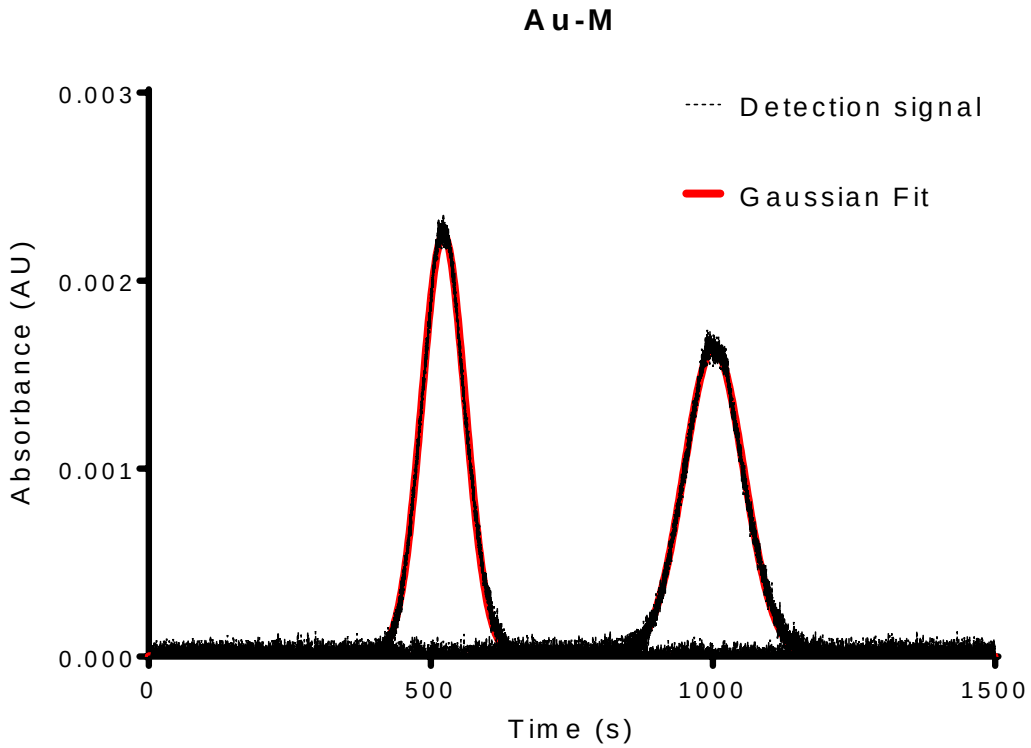

S10 Taylorgram and Gaussian fit of Au-M sample, measured at 520 nm.

TEM Analysis and Histograms:

The following histograms were gathered from analysing a minimum of 200 particles per sample (with the exception of the Au-S particles, where only 50 particles were counted). The histograms are normalized towards setting the total probability to 1.

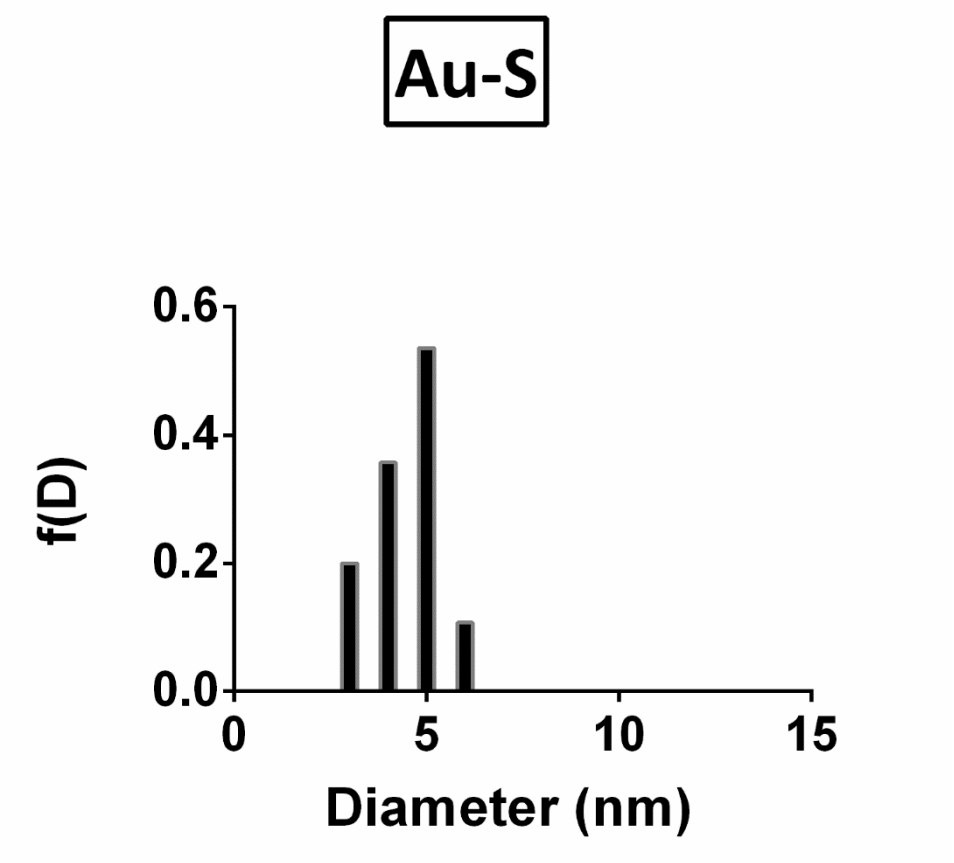

S11 TEM histogram of the Au-S nanoparticles.

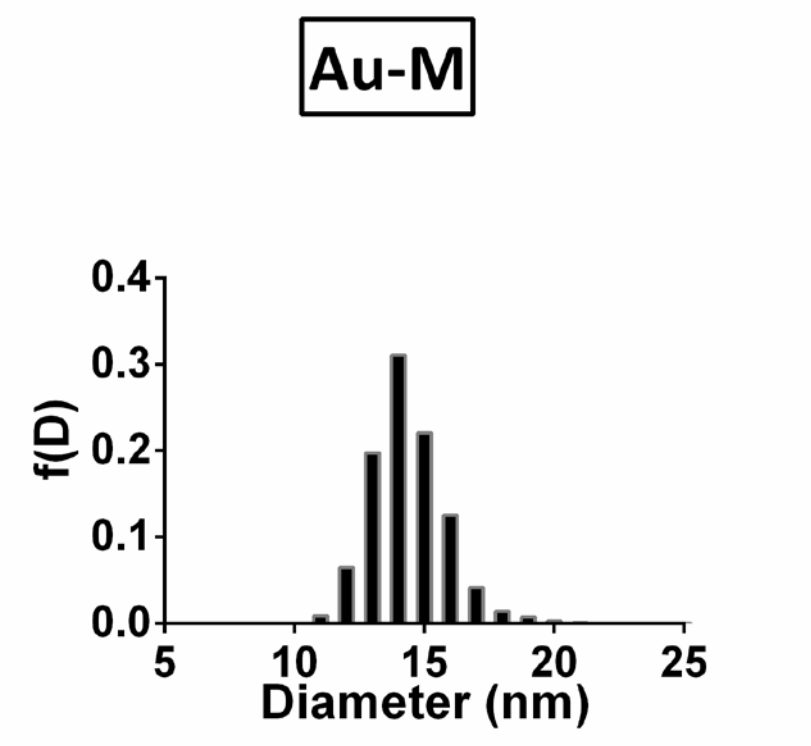

S12 TEM histogram of the Au-M nanoparticles.

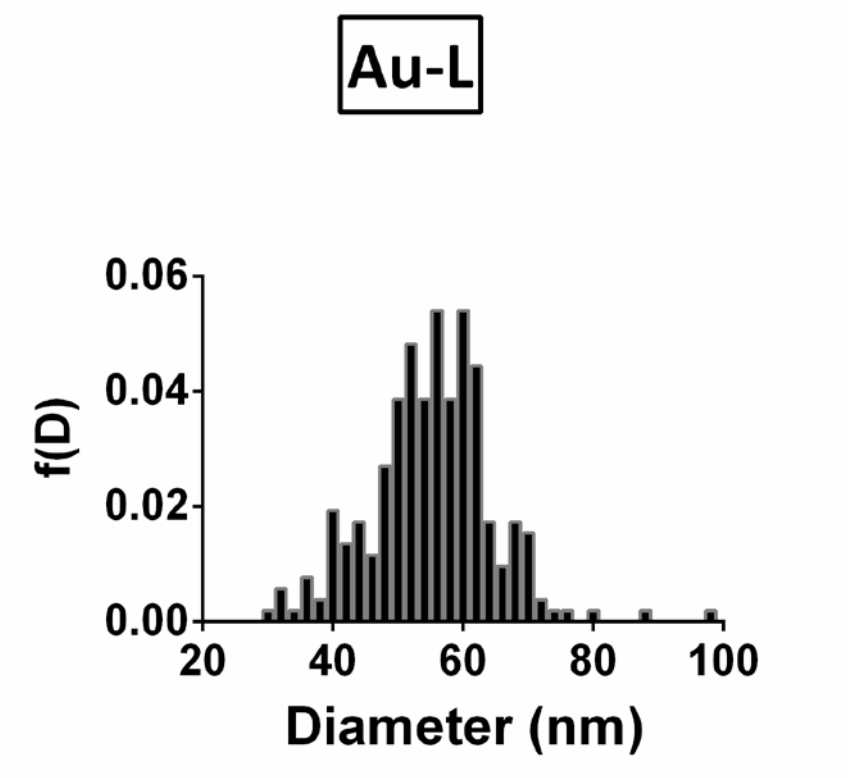

S13 TEM histogram of the Au-L nanoparticles.

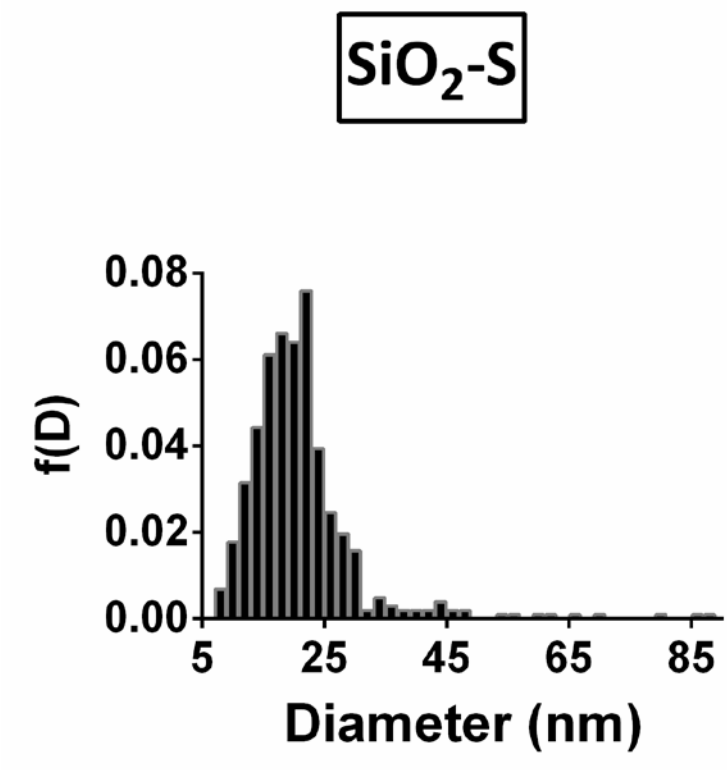

S14 TEM histogram of the SiO2-S nanoparticles.

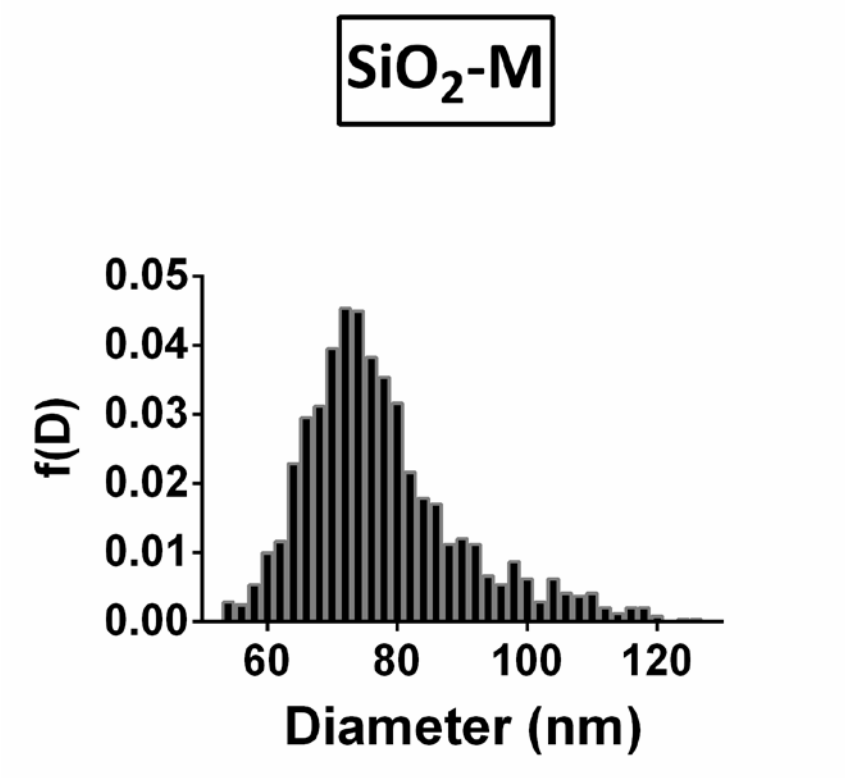

S15 TEM histogram of the SiO2-M nanoparticles.

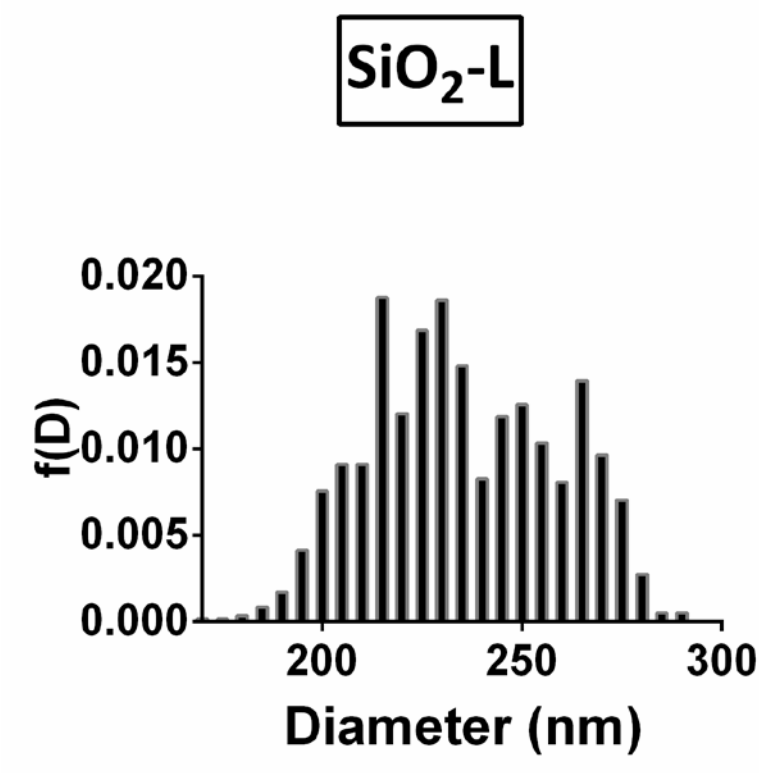

S16 TEM histogram of the SiO2-L nanoparticles.

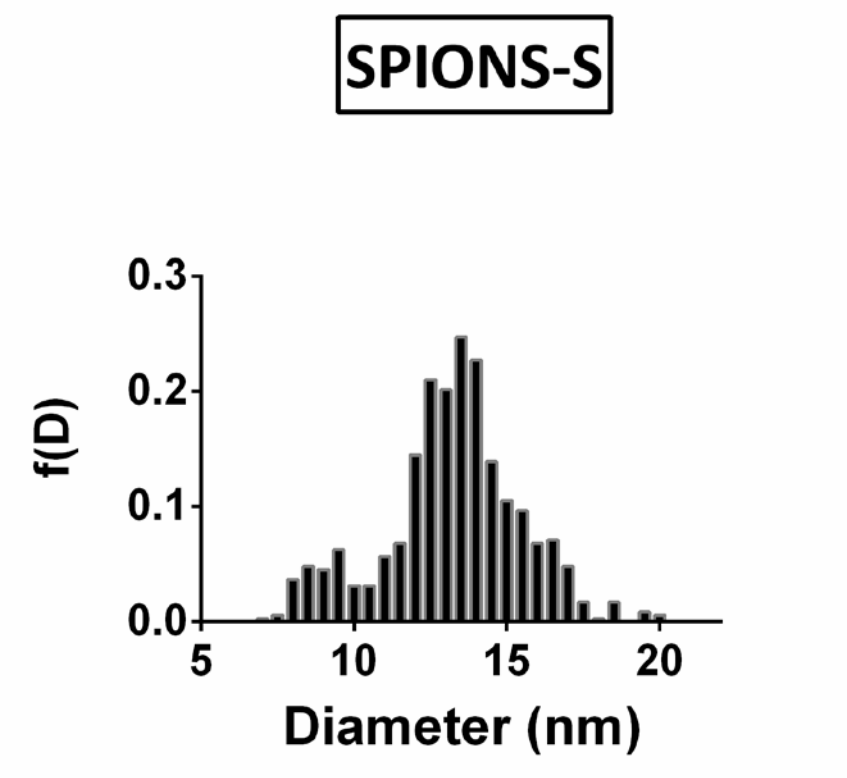

S17 TEM histogram of the SPIONS-S nanoparticles.

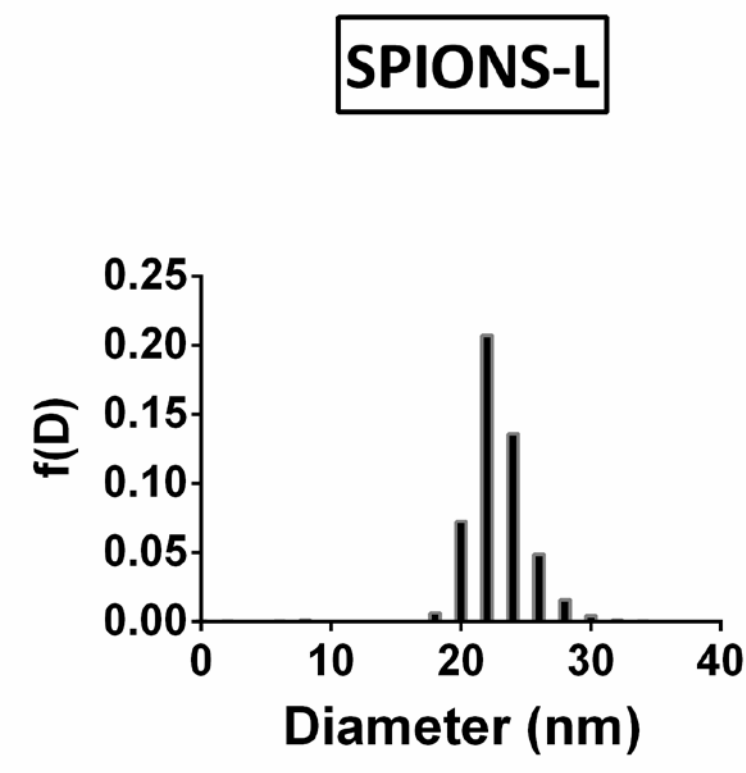

S18 TEM histogram of the SPIONS-L nanoparticles.

Dynamic light scattering results:

The following graphs show exemplary data gathered from characterizing the particles using dynamic light scattering. On the left hand side we show the correlation function and on the right hand side we show the recorded intensity fluctuations during the measurement.

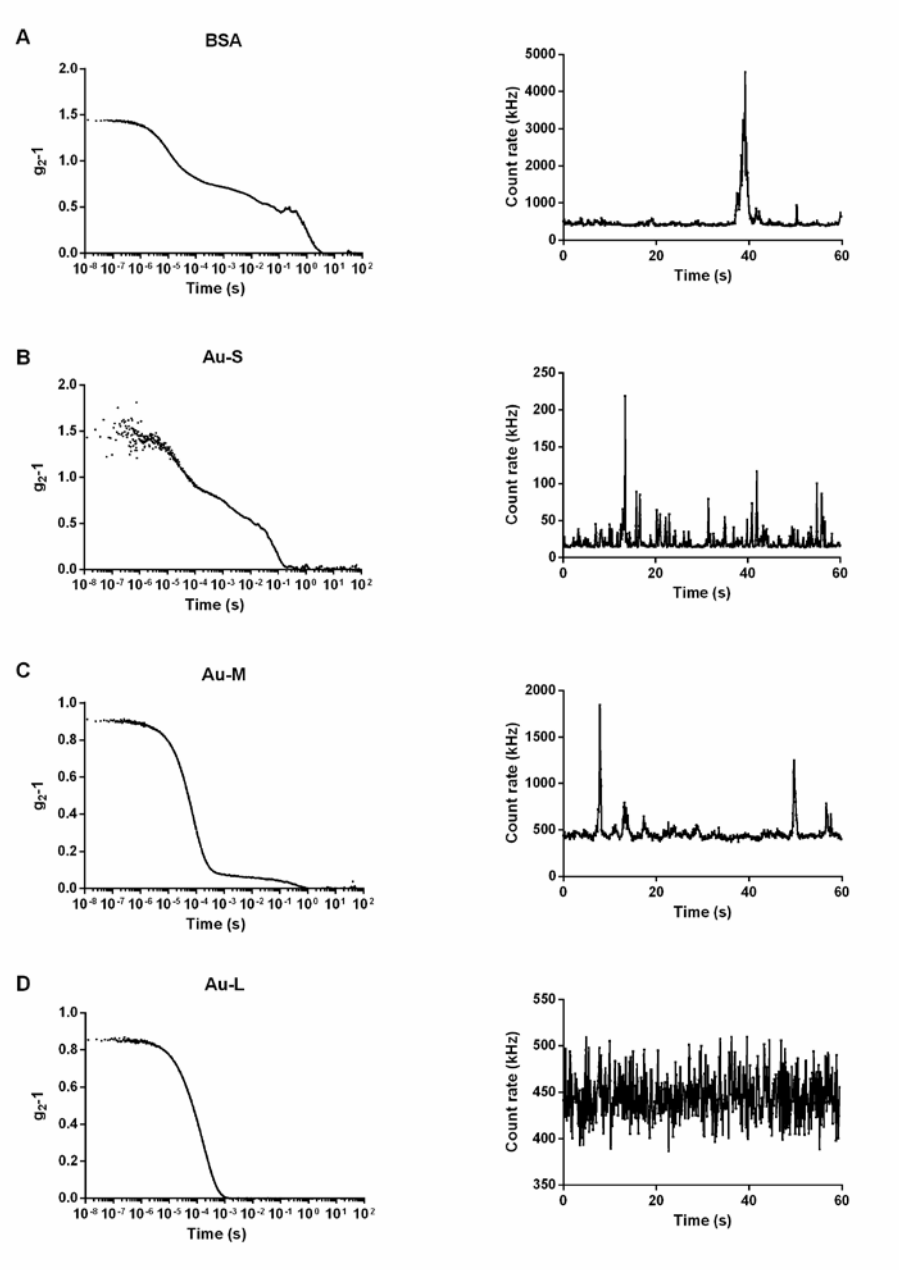

S19 Correlation functions and respective intensity fluctuations gathered during dynamic light scattering measurements of the following particles : A Bovine serum albumin (BSA); B Au-S; C Au-M and D Au-L.

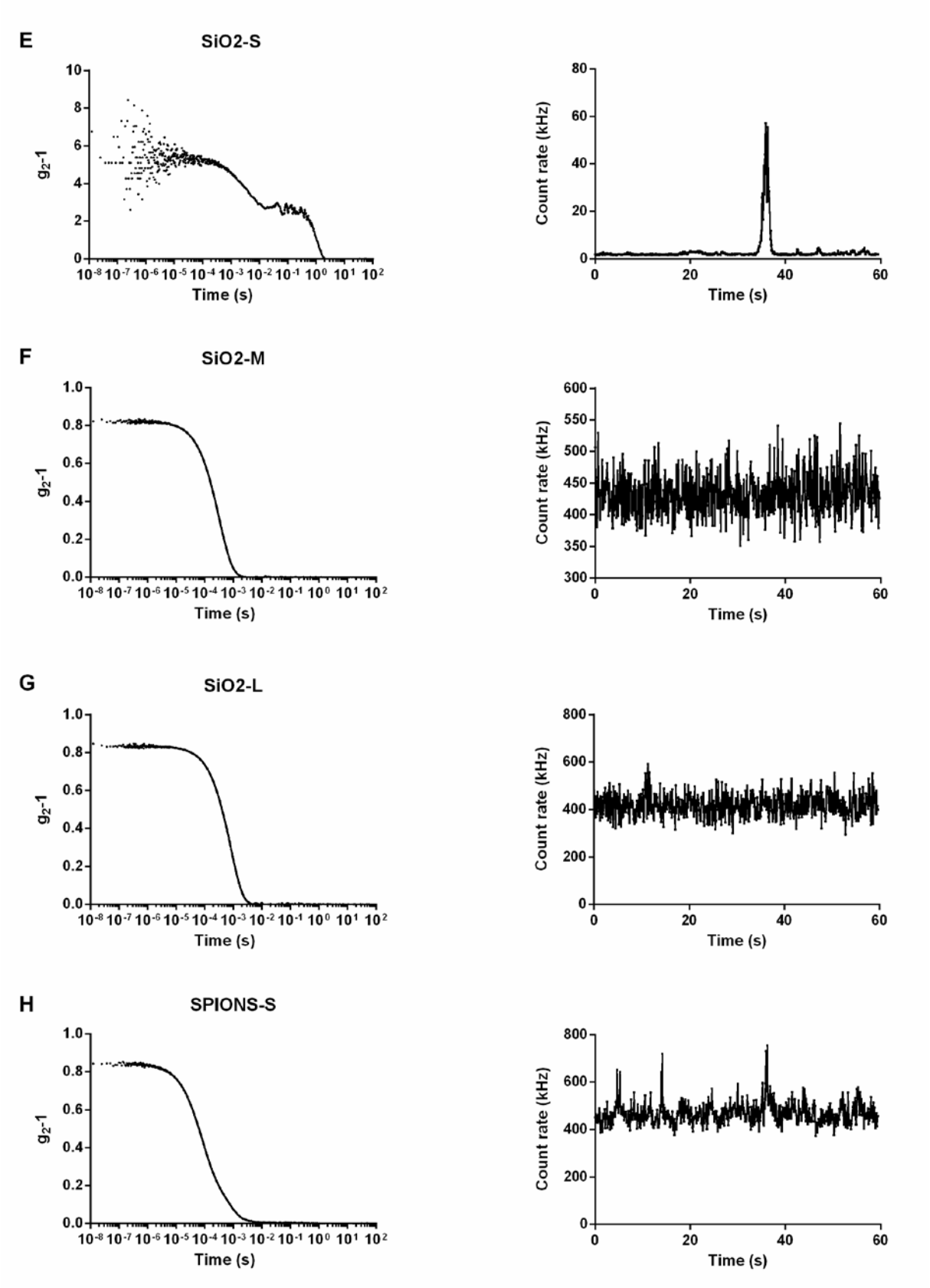

S20 Correlation functions and respective intensity fluctuations gathered during dynamic light scattering measurements of the following particles : E SiO2-S; F SiO2-M; G SiO2-L; H SPIONS-S.

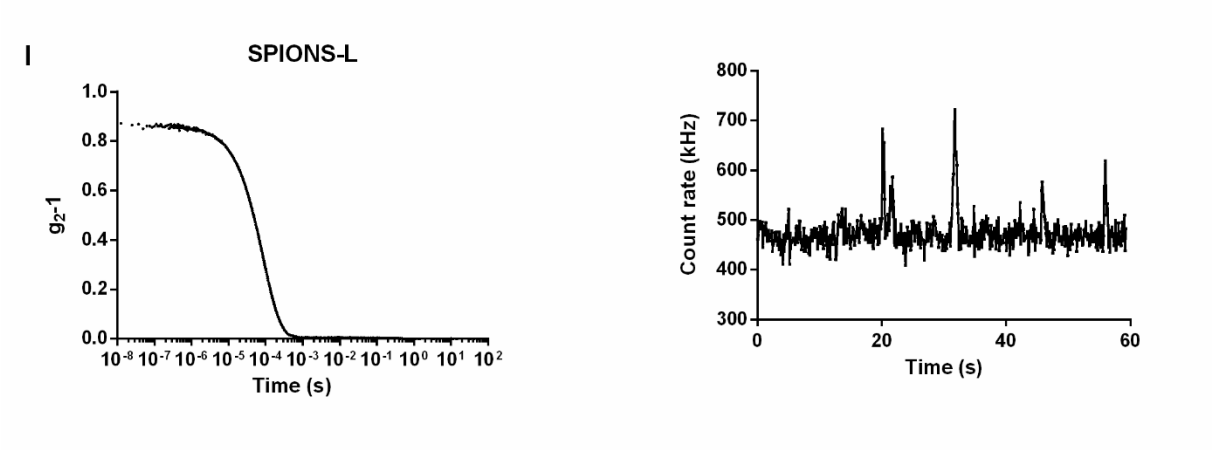

S21 Correlation functions and respective intensity fluctuations gathered during dynamic light scattering measurements of the following particles: I SPIONS-L.

S22 References.

[1] J. Turkevich, P.C. Stevenson, J. Hillier, A study of the nucleation and growth processes in the synthesis of colloidal gold, Discuss. Faraday Soc. 11 (1951) 55-75.
[2] K.R. Brown, D.G. Walter, M.J. Natan, Seeding of Colloidal Au Nanoparticle Solutions. 2. Improved Control of Particle Size and Shape, Chem. Mater. 12 (2000) 306-313.
[3] K.-T. Yong, Y. Sahoo, M.T. Swihart, P.N. Prasad, Synthesis and plasmonic properties of silver and gold nanoshells on polystyrene cores of different size and of gold–silver core–shell nanostructures, Colloids and Surfaces A: Physicochemical and Engineering Aspects 290(1-3) (2006) 89-105.
[4] J. Park, K. An, Y. Hwang, J.-G. Park, H.-J. Noh, J.-Y. Kim, J.-H. Park, N.-M. Hwang, T. Hyeon, Ultra-large-scale syntheses of monodisperse nanocrystals, Nat Mater 3(12) (2004) 891-5.
[5] M. Lattuada, T.A. Hatton, Functionalization of monodisperse magnetic nanoparticles, Langmuir 23 (2007) 2158-2168.
[6] K.D. Hartlen, P.T. Athanasopoulos, V. Kitaev, Facile Preparation of Highly Monodisperse Small Silica Spheres (15 to >200 nm) Suitable for Colloidal Templating and Formation of Ordered Arrays, Langmuir 5(24) (2008) 1714-1720.
[7] H. Giesche, Synthesis of Monodispersed Silica Powders I. Particle Properties and Reaction Kinetics, Journal of the European Ceramic Society (14) (1994) 189-204.
[8] B. Michen, C. Geers, D. Vanhecke, C. Endes, B. Rothen-Rutishauser, S. Balog, A. Petri-Fink, Avoiding drying-artifacts in transmission electron microscopy: Characterizing the size and colloidal state of nanoparticles, Sci Rep 5 (2015) 9793.
[9] G. Taylor, Dispersion of Soluble Matter in Solvent Flowing Slowly through a Tube, Proceedings of the Royal Society of London Series A-Mathematical and Physical Sciences 219(1137) (1953) 186-203.
[10] G. Taylor, Conditions under Which Dispersion of a Solute in a Stream of Solvent can be Used to Measure Molecular Diffusion, Proceedings of the Royal Society of London Series A-Mathematical and Physical Sciences 225(1163) (1954) 473-477.
[11] R. Aris, On the Dispersion of a Solute in a Fluid Flowing through a Tube, Proceedings of the Royal Society of London Series A-Mathematical and Physical Sciences 235(1200) (1956) 67-77.
[12] A. Alizadeh, C.A. Nieto de Castro, W.A. Wakeham, The Theory of the Taylor Dispersion Technique for Liquid Diffusivity measurements, International Journal of Thermophysics 1(3) (1980) 243-284.
[13] M.S. Bello, R. Rezzonico, P.G. Righetti, Use of Taylor-Aris Dispersion for Measurement of a Solute Diffusion Coefficient in Thin Capillaries, Science 266 (1994) 773-776.
[14] B.M. Belongia, J.C. Baygents, Measurements on the diffusion coefficient of colloidal Particles by Taylor Aris Dispersion, Journal of Colloid and Interface Science 195(1) (1997) 19 - 31.
[15] F. d'Orlye, A. Varenne, P. Gareil, Determination of nanoparticle diffusion coefficients by Taylor dispersion analysis using a capillary electrophoresis instrument, J Chromatogr A 1204(2) (2008) 226-32.
[16] L. Cipelletti, J.P. Biron, M. Martin, H. Cottet, Polydispersity analysis of Taylor dispersion data: the cumulant method, Anal Chem 86(13) (2014) 6471-8.
[17] L. Cipelletti, J.P. Biron, M. Martin, H. Cottet, Measuring arbitrary diffusion coefficient distributions of nano-objects by taylor dispersion analysis, Anal Chem 87(16) (2015) 8489-96.
[18] M. Höldrich, S. Liu, M. Epe, M. Lammerhofer, Taylor dispersion analysis, resonant mass measurement and bioactivity of pepsin-coated gold nanoparticles, Talanta 167 (2017) 67-74.